Surface Review and Letters, Vol. 9, No. 1 (2002) 515–520

FEASIBILITY STUDIES OF THE THREE-DIMENSIONAL DETECTOR FOR SOFT X-RAY EMISSION SPECTROSCOPY

M. OURA, K. KOBAYASHI,* M. WATANABE and Y. HARADA
RIKEN/SPring-8, 1-1-1 Kouto, Mikazuki-cho, Sayo-gun, Hyogo 679-5148, Japan

T. SUZUKI†
JASRI/SPring-8, 1-1-1 Kouto, Mikazuki-cho, Sayo-gun, Hyogo 679-5198, Japan

S. SHIN
Institute of Solid State Physics, University of Tokyo, Kashiwanoha, Kashiwa-shi, Chiba 277-8581, Japan
RIKEN/SPring-8, 1-1-1 Kouto, Mikazuki-cho, Sayo-gun, Hyogo 679-5148, Japan

O. JAGUTZKI
Institut für Kernphysik, Universität Frankfurt, August-Euler-Strasse 6, D-60486 Frankfurt, Germany

A time-resolving two-dimensional position-sensitive detector was applied to soft X-ray emission spectroscopy (SXES) and its feasibility was successfully studied by using synchrotron radiation. A soft X-ray emission spectrum synchronously acquired with bunch signal of the storage ring has elucidated that a threefold higher signal-to-noise ratio could at least be achieved. By adopting a pump–probe technique to SXES, we have preliminarily studied the effect of the electron–hole plasma (EHP) on the Si 2p soft X-ray emitting processes of Si crystal. A meaningful change in the excitation curve for the elastic scattering yields near the 2p thresholds was found to be probably due to the many-body interactions caused by the EHP.

1. Introduction

SXES using synchrotron radiation (SR) is a powerful tool[1–4] for studying the electronic structure of matter and the relaxation processes of excited states with a localized core hole. SXES also allows us to separate the angular momentum components of the valence states because of a clear selection rule due to the dipole nature of the X-ray transitions. Furthermore, since the mean free path of the soft X-rays is much longer than that of the electron, SXES enables us to study the electronic structure of bulk of the materials as well as the buried structure, such as the multiquantum well.

Recently, we have adopted a time-resolving two-dimensional (2D) position-sensitive detector,[5] i.e. 3D detector, to the SXE spectrometer in order to study the relaxation dynamics of the core hole states. Such a 3D detector has successfully demonstrated its feasibility for measuring charged particles in recoil ion momentum spectroscopy.[6,7] By utilizing a time sensitivity of the 3D detector for SXES, we expect we can pioneer new applications in spectroscopic studies. In the following sections, we briefly describe the experimental setup and preliminary results of the recent feasibility studies, in which SR-bunch gated SXES as well as SXES with simultaneous irradiation of SR and laser were carried out.

*Present address: JASRI/SPring-8, 1-1-1 Kouto, Mikazuki-cho, Sayo-gun, Hyogo 679-5198, Japan.
†Present address: Faculty of Environmental Engineering, The University of Kitakyushu, 1-1 Hibikino, Wakamatsu-ku, Kitakyushu, Fukuoka, 808-0135, Japan.

2. SXE Spectrometer with 3D Detector

The SXE spectrometer,[8] which is installed at the BL19B revolver–undulator beamline[9] of the Photon Factory (KEK), had been used for studying the solid state physics by means of SXES and resonant Raman scattering.[10,11] Figure 1 shows a schematic drawing of the SXE spectrometer equipped with the 3D detector. The details of the SXE spectrometer are given in Ref. 8; we describe here the 3D detector and its basic performance.

The 3D detector consists of a triple stack (Z-stack) of selected rimless microchannel plate (MCP) and a 2D position-sensitive delay line anode (helical wire pair). The typical performance and the characteristics of the 3D detector are summarized in Table 1. The position of the detected soft X-ray is independently encoded by the signal-arrival-time-difference at both ends for each parallel pair delay line. The four signal pairs from both delay line ends are fed into a differential amplifier by twisted-pair cables (equal length). The time sequence of the signals is measured by the time-to-digital converter (TDC), and the signal on the MCP back or front side is used as a time reference.

The surface of the front MCP of the Z-stack is coated by CsI in order to achieve enhanced soft X-ray quantum detection efficiency. In addition, a retarding wire mesh is mounted in front of the stack so that the secondary electrons ejected from CsI to the vacuum reflect back to the detector. Figure 2(a) represents the applied mesh-voltage dependence of the SXE yields of 100 eV photons and clearly shows the negative bias against the MCP front drastically increase the detection efficiency. Figure 2(b), on the other hand, shows the mesh-voltage dependence of the widths of the time- and position-spectrum. The time-spectrum was obtained using the signal on the MCP front and the bunch signal of the storage ring. The timing resolution became worse significantly when the mesh-voltage was close to that of the MCP front in contrast to the weak

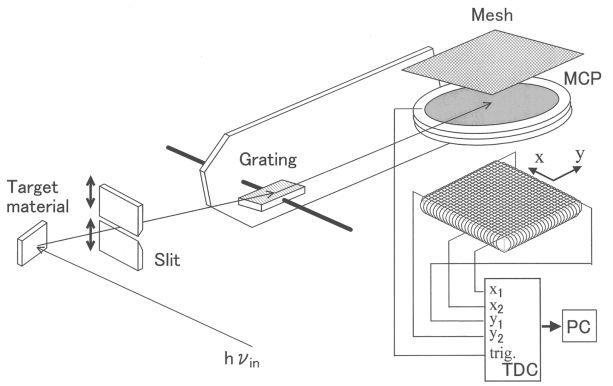

Fig. 1. Schematic drawing of the SXE spectrometer equipped with the 3D detector.

Table 1. Typical performance and characteristics of the 3D detector used as a photon detector for the time-sensitive SXES.

Position resolution	< 100 μm
Timing resolution	~ 500 ps
Overall linearity	200 μm
Rate capability	1 MHz
Multihit pulse pair resolution	10 ns
Active diameter	83 mm
Operating temperature range	-50 to 70°C
Operating pressure	$< 2 \times 10^{-4}$ Pa

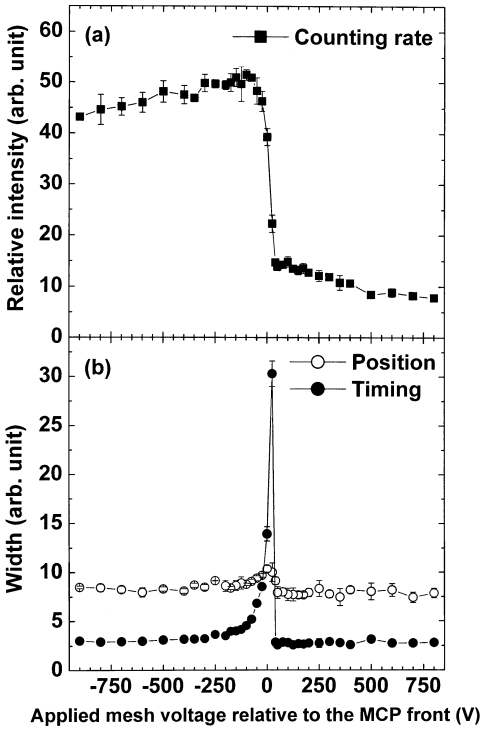

Fig. 2. Applied mesh-voltage dependence of (a) the SXE yield and (b) the widths of the time- and the position-spectrum.

mesh-voltage dependence of the position resolution. From these dependences, we found that the negative mesh-voltage of several hundred eV relative to the MCP front gives rise to higher quantum efficiency with reasonable timing resolution for the soft X-ray detection.

3. Feasibility Experiments

In this study, we have employed ZnSe and Si crystals as target materials. ZnSe target was chosen to test a feasibility of SR-bunch gated SXES by measuring the weak satellite structure due to the shake processes[12,13] in the $L_{2,3}$ emission spectrum of Zn. On the other hand, Si target was used to explore new applications in spectroscopic studies by means of SXES with simultaneous irradiation of SR and laser.

Experiments were performed at the Photon Factory during a single-bunch operation of the storage ring. The SXE spectra were excited by photons from the VLM19 monochromator[14] with a varied-line spacing plane grating. The energy of the photon beam was set to 1072 eV for ZnSe and 98–103 eV for Si, respectively.

The SXE spectrometer was tuned using the fluorescence emitted from the standard sample. The grating had 1200 grooves/mm. The 3D detector was oriented at the correct position on the relevant Rowland circle by adjusting the computer-controlled actuators. The $L_{2,3}$ emission spectra of Zn were recorded in second order diffraction and those of Si were acquired with the geometry of first order diffraction.

4. Results and Discussion

4.1. *SR-bunch gated SXES*

If we could achieve further enhancement in the signal-to-noise (S/N) ratio for the soft X-ray detection, an observation of the very weak transition is expected to become possible. Such a situation gives rise to opportunities to study the multielectron processes by measuring the weak satellite lines.[12,13]

With the advent of the recent synchrotron radiation sources, measuring an evolution of the intensities for shake processes especially near their threshold has become possible.[15–18] Such systematic studies will give us deeper insight into understanding the dynamic electron–electron correlations in photoionization processes.

Figure 3 shows the timing spectrum of which prompt peak represents the SR-arrival time. By adopting the information of the SR-bunch signal[19]

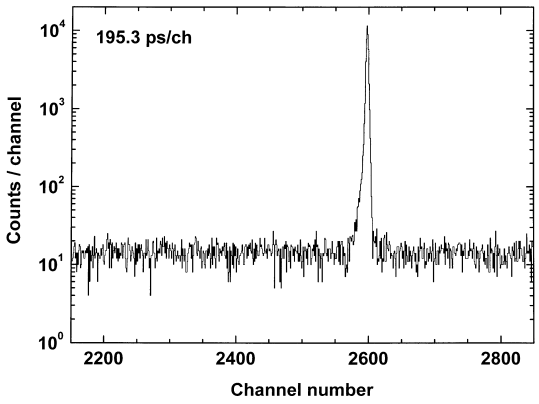

Fig. 3. Timing spectrum obtained using the signal on the MCP front and the bunch signal of the storage ring.

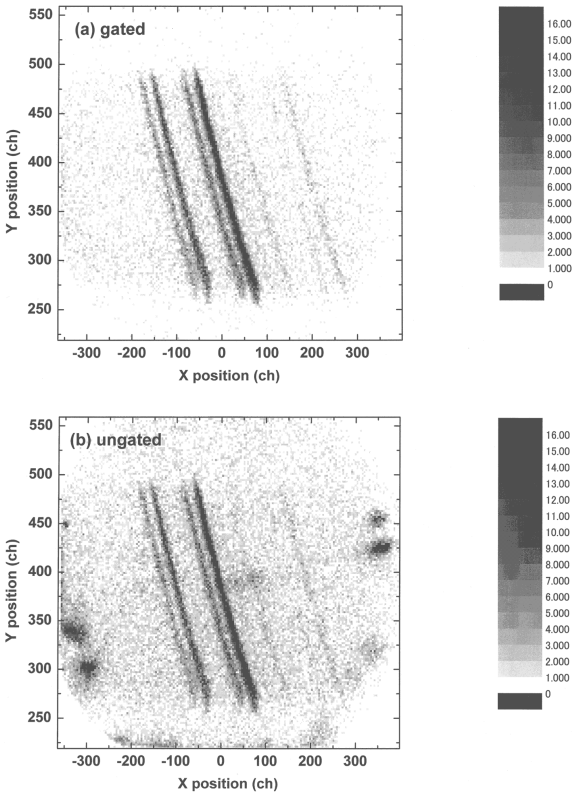

Fig. 4. Two-dimensional position spectra of the wavelength dispersed Zn 2p fluorescence in the condition of (a) gated and (b) ungated.

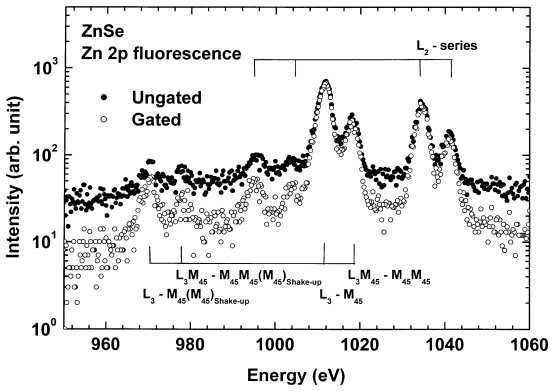

Fig. 5. SXE spectra emitted from 2p-excited Zn of the ZnSe target. Open circles show SR-bunch gated SXE spectrum and closed circles represent ungated spectrum. In the spectrum, characteristic diagram lines of Zn and some satellite lines emitted in the multielectron processes are clearly resolved.

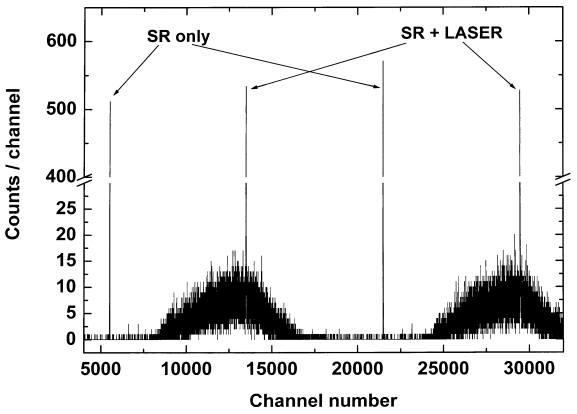

Fig. 6. Timing spectrum obtained in the condition of laser and SR coirradiation. Sharp peaks represent the SR-arrival time and the broad structures show the laser irradiation. The time difference of each SR peak is about 624 ns.

to this spectrum we deconvoluted the timing resolution of our 3D detector to be 550 ps. We could easily acquire the SR-bunch gated spectrum by using this prompt bunch structure.

In Fig. 4, we compare the 2D position spectra obtained with and without gating. Figure 4(a) clearly shows the benefit of SR-bunch gated SXES in which most of the random noise, especially several remarkable "hot spots" shown in Fig. 4(b), was suppressed. Accordingly we could achieve an at least threefold higher S/N ratio in the final spectrum, as shown in Fig. 5. As can be seen in the spectrum, strong satellite lines originating from the decay of $L_{2,3}$ core holes in the presence of a spectator 3d vacancy (denoted as $L_3M_{4,5}$–$M_{4,5}M_{4,5}$ in the figure) were clearly resolved from the diagram lines (L_3–$M_{4,5}$). On the low-energy side of these strong lines, the gated spectrum has manifested its visibility in the region of the weak satellite structure associated with the final-state shakeup [denoted as L_3–$M_{4,5}(M_{4,5})_{\mathrm{shakeup}}$ and $L_3M_{4,5}$–$M_{4,5}M_{4,5}(M_{4,5})_{\mathrm{shakeup}}$] processes.

Accordingly, the SR-bunch gated SXES elucidates its feasibility in the study of weak multielectron processes. It will be a powerful tool for studying the threshold phenomena.

4.2. *SXES with simultaneous irradiation of SR and laser*

In order to explore new applications in spectroscopic studies by means of SXES, a pump–probe technique was applied using compact semiconductor laser (5 W). The pulsed laser beam was tuned so as to irradiate the target material of high-purity FZ-grown Si crystal in synchronous with the SR.

Figure 6 shows the TDC spectrum, observed in the condition of 2-SR × 1-laser configuration, in which sharp peaks represent the SR-arrival time and the broad structures exhibit the laser irradiation. The laser beam was focused using a lens system onto the sample surface giving rise to a high power density. The density of the exciton was roughly estimated to be larger than 10^{18} $\mathrm{cm}^{-3}\mathrm{pulse}^{-1}$. The temperature of the sample was measured to be about 40 K. Therefore it is expected to form a pure EHP when the laser beam is "on." The existence of such high density exciton will screen the elastic scattering when the incident photon energy approaches the conduction band edge.

We compared the SXE spectra obtained in the conditions with laser beam "on" and "off." We, however, could scarcely observe a meaningful difference between two spectra caused by the laser irradiation, probably due to the existence of the lower-density condensed plasma (CP), since the lifetime of such high density EHP is long enough ($\sim$ 150 ns)[20] to survive as CP when the laser beam is "off."

We therefore compare the present excitation curves for the elastic scattering yields and the fluorescence yields for the Si 2p region with those obtained previously.[10] Figure 7(a) was obtained by

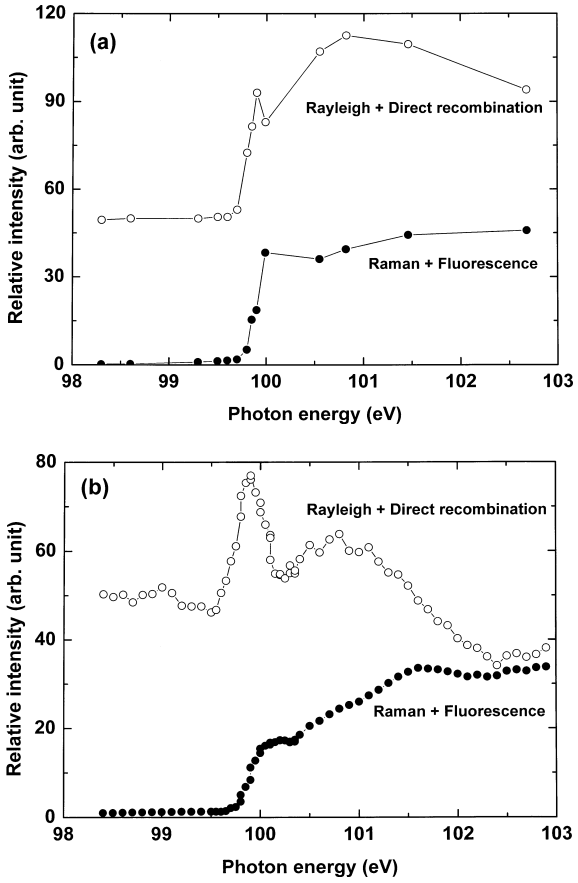

Fig. 7. Photon energy dependence of the intensities of the elastic scattering and the fluorescence near the Si 2p thresholds for (a) ordinary SXES[10] and (b) SXES with laser irradiation.

means of ordinary SXES while Fig. 7(b) represents the preliminary results obtained by the present studies. The spectrum seems to show a meaningful change in the intensity of the elastic scattering yields in the case of laser "on," which is probably due to the effect of the EHP. Furthermore, the present result for the elastic scattering yields exhibits a weak structure around 99 eV which is close to the valence-band top. There might exist unoccupied states at the valence band top due to the EHP. A rigorous study is in progress.

5. Conclusions

A time-resolving two-dimensional position-sensitive detector was successfully applied to SXES and its feasibility was studied by using synchrotron radiation. A SXE spectrum synchronously acquired with SR-bunch signal has elucidated that a threefold higher S/N ratio could be achieved. Combining the pump–probe technique with SXES, the effect of the high density exciton on the soft-X-ray-emitting processes was preliminarily studied and a meaningful change in the intensity of the elastic scattering was found to be probably due to the existence of the high-density exciton.

Acknowledgment

The authors would like to thank Mrs Akiko Fukushima of the Institute of Solid State Physics, University of Tokyo, for her help during the experiments.

References

1. T. A. Callcott, K. L. Tsang, C. H. Zhang, D. L. Ederer and E. T. Arakawa, *Rev. Sci. Instrum.* **57**, 2680 (1986).
2. J. Nordgren, G. Bray, S. Cramm, R. Nyholm, J.-E. Rubensson and N. Wassdahl, *Rev. Sci. Instrum.* **60**, 1690 (1989).
3. J. Nordgren, *New Directions in Research with Third-Generation Soft X-Ray Synchrotron Radiation Sources*, eds. A. S. Schlachter and F. J. Wuilleumier (Kluwer, Dordrecht, 1994), p. 189; D. L. Ederer, K. E. Miyano, W. L. O'Brien, T. A. Callcott, Q.-Y. Dong, J. J. Jia, D. R. Mueller, J.-E. Rubensson, R. C. C. Perera and R. Shuker, *ibid.*, p. 281.
4. A. Kotani and S. Shin, *Rev. Mod. Phys.* **73**, 203 (2001).
5. Fast position- and time-sensitive MCP detectors manufactured by RoentDek, Handels GmbH, Im Vogelshaag 8, D-65779 Kelkheim, Germany.
6. R. Dörner, T. Vogt, V. Mergel, H. Khemliche, S. Kravis, C. L. Cocke, J. Ullrich, M. Unverzagt, L. Spielberger, M. Damrau, O. Jagutzki, I. Ali, B. Weaver, K. Ullmann, C. C. Hsu, M. Jung, E. P. Kanter, B. Sonntag, M. H. Prior, E. Rotenberg, J. Denlinger, T. Warwick, S. T. Manson and H. Schmidt-Böcking, *Phys. Rev. Lett.* **76**, 2654 (1996).
7. V. Mergel, R. Dörner, M. Achler, Kh. Khayyat, S. Lencinas, J. Euler, O. Jagutzki, S. Nüttgens, M. Unverzagt, L. Spielberger, W. Wu, R. Ali, J. Ullrich, H. Cederquist, A. Salin, C. J. Wood, R. E. Olson, Dž. Belkic, C. L. Cocke and H. Schmidt-Böcking, *Phys. Rev. Lett.* **79**, 387 (1997).
8. S. Shin, A. Agui, M. Fujisawa, Y. Tezuka, T. Ishii and N. Hirai, *Rev. Sci. Instrum.* **66**, 1584 (1995).
9. G. Isoyama, S. Yamamoto, T. Shioya, J. Ohkuma, S. Sasaki, T. Mitsuhashi, T. Yamakawa and H. Kitamura, *Rev. Sci. Instrum.* **60**, 1863 (1989).

10. S. Shin, A. Agui, M. Watanabe, M. Fujisawa, Y. Tezuka and T. Ishii, *Phys. Rev.* **B53**, 15660 (1996).
11. S. Shin, A. Agui, M. Watanabe, M. Fujisawa, Y. Tezuka and T. Ishii, *J. Electron Spectrosc. Relat. Phenom.* **79**, 125 (1996).
12. N. Wassdahl, J.-E. Rubensson, G. Bray, P. Glans, P. Bleckert, R. Nyholm, S. Cramm, N. Mårtensson and J. Nordgren, *Phys. Rev. Lett.* **64**, 2807 (1990).
13. M. Magnuson, N. Wassdahl and J. Nordgren, *Phys. Rev.* **B56**, 12238 (1997).
14. M. Fujisawa, A. Harasawa, A. Agui, M. Watanabe, A. Kakizaki, S. Shin, T. Ishii, T. Kita, T. Harada, Y. Saitoh and S. Suga, *Rev. Sci. Instrum.* **67**, 345 (1996).
15. M. Deutsch, O. Gang, K. Hämäläinen and C. C. Kao, *Phys. Rev. Lett.* **76**, 2424 (1996).
16. M. Fritsch, C. C. Kao, K. Hämäläinen, O. Gang, E. Förster and M. Deutsch, *Phys. Rev.* **A57**, 1686 (1998).
17. C. Sternemann, A. Kaprolat, M. H. Krisch and W. Schülke, *Phys. Rev.* **A61**, 020501 (R) (2000).
18. R. Diamant, S. Huotari, K. Hämäläinen, C. C. Kao and M. Deutsch, *Phys. Rev. Lett.* **84**, 3278 (2000); *Phys. Rev.* **A62**, 052519 (2000).
19. T. Obina, private communications.
20. L. M. Smith and J. P. Wolfe, *Phys. Rev.* **B51**, 7521 (1995).